Organic & Biomolecular Chemistry

ROYAL SOCIETY OF CHEMISTRY

PAPER

View Article Online
View Journal | View Issue

Check for updates

Cite this: *Org. Biomol. Chem.*, 2022, **20**, 7981

The role of indolyl substituents in squaramide-based anionophores†

Giacomo Picci,[a] Israel Carreira-Barral,[b] Daniel Alonso-Carrillo,[b] Chiara Busonera,[a] Jessica Milia,[a] Roberto Quesada *[b] and Claudia Caltagirone *[a]

Received 8th August 2022,
Accepted 23rd September 2022

DOI: 10.1039/d2ob01444k

rsc.li/obc

A new family of squaramide-based anionophores (**L1–L8**) have been synthesised and fully characterised with the aim to investigate the effect of indolyl substituents on their anion binding and transmembrane transport properties. **L1**, **L2**, **L6**, and **L8**, bearing a 7-indolyl/indol-7-yl moiety as the substituent, were found to be the most efficient of the series in binding chloride with high stability constants. **L1**, **L6**, and **L8** were also found to be the most potent anionophores of the series, able to mediate transmembrane anion transport. In particular, **L6** bearing the 3,5-bis(trifluoromethyl)phenyl group was found to be the most active transporter, and its efficiency as an anionophore/anion transporter was favourably compared with that of their symmetrically-substituted squaramide analogues **L9** and **L10**, previously reported in the literature.

Introduction

Chloride is the most abundant anion in the human body and plays important roles in various biological and cellular processes such as control of the membrane potential, cell volume, cellular pH balance or secretion of the transepithelial fluid and electrolytes.[1,2] Indeed, misregulation of chloride transport could lead to a range of diseases.[3] One of these conditions is cystic fibrosis (CF). Cystic fibrosis originates from mutations of the CF transmembrane conductance regulator (*CFTR*) gene which encodes for the transmembrane transport protein CFTR- that selectively transports Cl^- and HCO_3^- in epithelial tissues.[4] The resulting clinical manifestations are diverse and multi-organ, affecting especially the lungs, and the gastrointestinal and endocrine systems.[5] Interventions at the root of the problem through pharmacological modulation of CFTR production and activity have just opened a whole new scenario for improved life-quality of affected patients.[6] In this context, the development of synthetic chloride carriers or channels that could act as a replacement of defective natural chloride channels has attracted the interest of researchers.[7–10] Disruption of chloride transport and homeostasis upsetting could lead to cellular stress and cytotoxicity.[11] This is an area in which anion selective ionophores, anionophores, are being explored as future anticancer drugs,[12–15] antimicrobials or antiparasitic agents.[16–18] The development of these applications relies on understanding the multiple factors that play a role in determining the efficiency of these molecules as anion carriers.[19] In particular, various studies have demonstrated the important role of the lipophilicity of the carrier to improve the partitioning into the lipid membrane and increase the transport ability.[20,21] Synthetic chloride carriers should be able to extract the anion from aqueous phases and facilitate its diffusion through the apolar membrane interior.[22–25] This implies that the carrier should form a stable adduct with chloride. For this reason, classic anion binding motifs such as ureas, thioureas, amides, and squaramides have been successfully used for developing artificial chloride carriers.[26–29] In particular, we have recently demonstrated that the use of additional H-bond donor groups, such as indole, into the molecular skeleton in the design of squaramide-based anion receptors could be an alternative to the introduction of electron-withdrawing groups (EWGs, such as $-CF_3$ and $-NO_2$) to obtain potent anionophores that can also work in aqueous media.[30] On this basis, we decided to investigate the effect on the anion transport abilities of non-symmetric squaramides of replacing one of the indole moieties in the previously reported bis-indolyl squaramide with different substituents such as 4-pentafluorosulfanylphenyl (**L1**), *n*-hexyl (**L2**), tryptamine (**L3**), 3,5-bis(trifluoromethyl)phenyl (**L6**), and trifluomethyl coumarin (**L8**) (Scheme 1). We also explored the effect on the transport properties of changing the position of the indole NH with respect

[a]*Dipartimento di Scienze Chimiche e Geologiche, Università degli Studi di Cagliari, S.S. 554 Bivio per Sestu, 09042 Monserrato (CA), Italy. E-mail: ccaltagirone@unica.it*
[b]*Departamento de Quimica, Facultad de Ciencias, Universidad de Burgos, 09001 Burgos, Spain. E-mail: rquesada@ubu.es*

†Electronic supplementary information (ESI) available. CCDC 2194712 (**L4**) and 2194745 (**L6**·TBACl). For ESI and crystallographic data in CIF or other electronic format see DOI: https://doi.org/10.1039/d2ob01444k

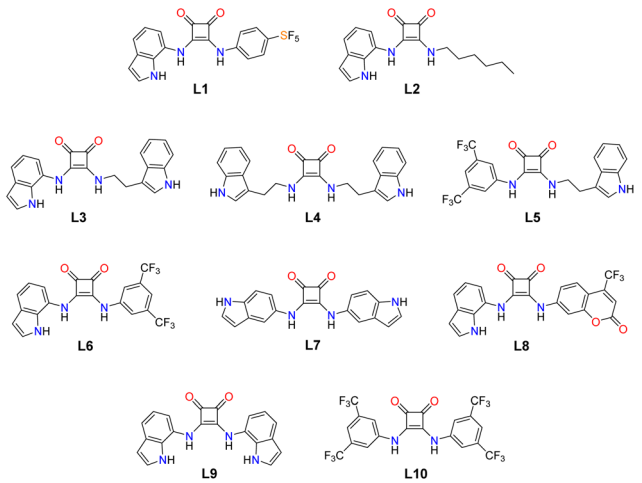

Scheme 1 Anionophores **L1–L8** discussed in this paper. **L9** and **L10** have been included in the study for comparative purposes.

to the cyclobutene ring by using tryptamine for the symmetric squaramide **L4** and for the non-symmetric squaramide **L5**, bearing 3,5-bis(trifluoromethyl)phenyl as a second substituent, and 5-aminoindole for **L7** (Scheme 1). Solid state and solution studies were carried out to evaluate the interaction of these receptors with chloride, whereas anion transport experiments in model liposomes (POPC) were performed to explore the ability of this new family of indole-containing squaramide-based receptors to act as anionophores.

Results and discussion

Synthesis and characterisation of the compounds and solid-state studies

Squaramides **L1–L8** (Scheme 1) were synthesised following different reaction sequences depending on their symmetry and on the nature of their substituents. In the case of symmetric squaramides (**L4** and **L7**), the reaction between diethyl squarate and the corresponding amine (2 equiv.) in the presence of $Zn(OTf)_2$ as a Lewis acid catalyst provided the desired compounds. For the non-symmetric squaramides, an intermediate containing one of the substituents was first synthesised from diethyl squarate and the appropriate amine, employing an excess of the squarate. Once isolated, the second residue was introduced by the reaction between such an intermediate and the desired amine; in all cases, the presence of the Zn(II) catalyst was necessary to allow the reaction. Compounds **L1–L8** were obtained in satisfactory to good yields (50–81%) and fully characterised (^{1}H and ^{13}C NMR spectroscopy, high-resolution mass spectrometry and, in some cases, single-crystal X-ray diffraction; see the ESI, for more details, Fig. S1–S34† for ^{1}H and ^{13}C NMR spectra, and high-resolution mass spectra).

Single crystals of **L6**·TBACl were grown by slow evaporation of an *n*-butanol solution containing **L6** and two equivalents of tetrabutylammonium chloride. The asymmetric unit consists of two 1 : 1 receptor : chloride adducts and two tetrabutylammonium cations. The receptor, which exhibits positional disorder in its two trifluoromethyl groups, interacts with the chloride anion through its three hydrogen-bond donor groups (see Fig. 1 for the structure of one of the two adducts). For both adducts, the distances between the N–H fragments of the squaramide core and the chloride anion [N···Cl 3.159–3.189 Å] are shorter than those found for the hydrogen bond involving the indole ring [N···Cl 3.221–3.311 Å], with N–H–Cl angles close to linearity in most of the cases (158.43–173.45°). The observed hydrogen-bonding interactions are of moderate strength, being those involving the indole N–H fragment the weaker ones. In fact, in one of the adducts found in the asymmetric unit, the indole ring is significantly bent with respect to the plane defined by the atoms of the squaramide core (the angle between this plane and that of the indole ring is 25.27°), whereas in the other adduct both fragments are almost coplanar (angle between planes: 6.38°). N-squaramide···Cl and N-indole···Cl distances are similar to those found in structurally related compounds.[30] The closest aromatic C–H fragment of the 3,5-bis(trifluoromethyl)phenyl residue to the chloride anion also establishes a weak hydrogen-bonding interaction. Meanwhile, parallel-displaced π-stacking interactions between the 3,5-bis(trifluoromethyl)phenyl substituents of contiguous receptor molecules are observed; the centroid–centroid distance for the stacked aromatic rings is 3.811 Å, whereas the closest C···C contact is 3.694 Å (Fig. S38†). Hydrogen bond distances and angles for **L6**·TBACl and crystal data and refinement details of both structures can be found in Tables S1 and S2,† respectively.

Altogether, this result provides evidence for a convergent hydrogen-bond cleft that is suitable for interaction with halide anions, not only in the solid state but also in solution (*vide infra*).

Solution studies

Anion-binding studies towards chloride and nitrate anion species (as tetrabutylammonium salts) were conducted by means of ^{1}H-NMR titrations using DMSO-d_6/0.5% water as a

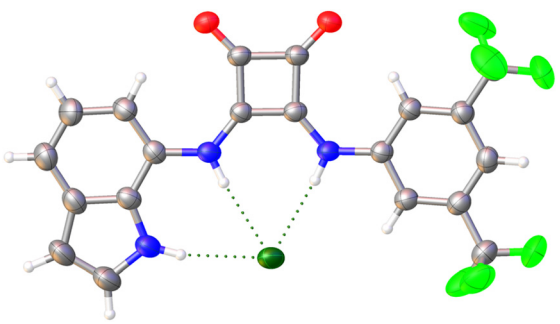

Fig. 1 X-ray structure of **L6**·TBACl. Only one of the two adducts found in the asymmetric unit is shown. Trifluoromethyl groups exhibit positional disorder, and the represented fluorine atoms correspond to those displaying the highest occupation factor. A tetrabutylammonium cation has been omitted for the sake of simplicity. The thermal ellipsoid plot (Olex 2) is at the 30% probability level.

solvent mixture. Stability constants from the obtained ^{1}H-NMR titration curves (see the ESI, Fig. S39–S64†) were calculated by fitting the data to a 1 : 1 binding model using WinEQNMR2.[31] The results are shown in Table 1.

As reported in Table 1, the calculated stability constants suggest how the presence of the indol-7-yl moiety in the structure of the studied squaramide-based receptors causes a strong interaction towards chloride species following the order **L6** > **L1**≡**L2**≡**L8** > **L3**. Indeed, as observed in the stack plot shown in Fig. 2 for the ^{1}H NMR titration conducted for **L6** in the presence of increasing amounts of TBACl, the signals attributable to the squaramide NH protons (in green and blue for the indolyl and 3,5-bis(trifluoromethyl)phenyl moieties, respectively) undergo a dramatic downfield shift (Δppm = 1.77 for the NH adjacent to the indolyl moiety, Δppm = 1.16 for the NH adjacent to the 3,5-bis(trifluoromethyl)phenyl moiety). The downfield shift of the signal corresponding to the indole NH protons (in red in Fig. 2) is less pronounced, with a Δppm of 0.20. A significant downfield shift was also observed for the doublet at *ca.* 7.2 ppm (Δppm = 0.36), which probably represents the formation of the strong H-bond between the squaramide NH groups and the anion guest. Interestingly, for all the 7-indolyl-containing squaramides (**L1–L3**, **L6**, and **L8**) a cooperativity of the squaramide core NHs and the 7-indolyl NHs in binding of the anion is observed. This behaviour is similar to that previously found for the symmetric 7-indolyl squaramide.[30]

Moreover, the experimental evidence observed in solution for all the 7-indolyl-containing squaramides is in agreement with the solid state structure of **L6**·TBACl (see above).

Furthermore, it is worth highlighting that no significant interactions of the indolyl group and the anion were detected in the case of **L4**, **L5**, and **L7**, underscoring how both the distance and the position of the indolyl NH binding site in the squaramide core are critical for contributing to the stabilization of the anion. Indeed, in **L4** and **L5**, bearing the tryptamine moiety as a substituent, the presence of the ethyl chain along with the lower convergence of the indolyl NH site is detrimental for the anion binding ability and the cooperativity between the two hydrogen-bond donor sites in binding the anion. On the other hand, in the case of **L7** it is the different position of the indolyl NH that caused a dramatic decrease of the binding capability towards chloride. Nevertheless, ^{1}H-NMR titration experiments using $TBANO_3$ showed very limited evidence of binding towards this anion and only minor shifts of N–H signals were observed (see the ^{1}H-NMR titrations paragraph in the ESI for details†).

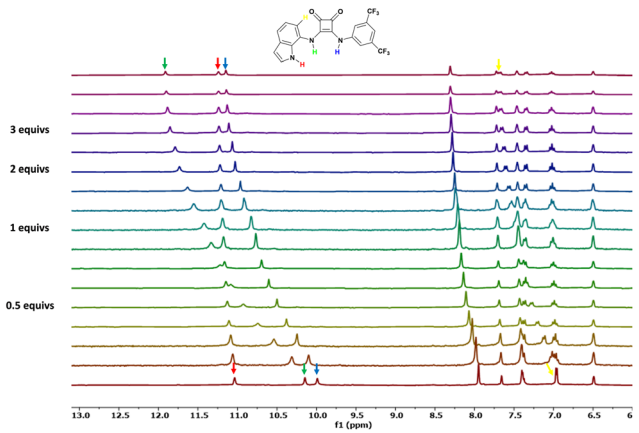

Fig. 2 Stack plot of the ^{1}H NMR spectra of **L6** upon addition of increasing amounts of TBACl in DMSO-d_6/0.5% water (298 K).

Transmembrane anion transport studies

The ability of **L1–L8** to facilitate the transmembrane anion transport was evaluated in model liposomes (1-palmitoyl-2-oleoyl-*sn-glycero*-3-phosphocoline, POPC) by potentiometric (ion-selective electrode, ISE) and fluorescence-based techniques. To perform ISE experiments, vesicles loaded with a NaCl aqueous solution buffered to pH 7.2 were suspended in an isotonic, chloride-free aqueous solution, also buffered to pH 7.2 (see the ESI for details, Fig. S65–S87†). Chloride efflux elicited by the addition of a compound (t = 0 s) at a certain concentration was recorded over time with a chloride-selective

Table 1 Association constants K_a for compounds **L1–L10** with chloride and nitrate (added as their tetrabutylammonium salts), determined from ^{1}H NMR titration experiments in DMSO-d_6/0.5% water at 298 K; transport activities expressed as EC_{50} and the Hill parameter (n); and calculated lipophilicities. All errors are ≤15%

Code	K_a (M^{-1}) Cl^-	Cl^-/NO_3^- antiport assay			Cl^-/HCO_3^- antiport assay			log P^a
		EC_{50} (nM)	EC_{50} (mol%)	n	EC_{50} (nM)	EC_{50} (mol%)	n	
L1	1000	132 ± 13	0.026 ± 0.003	1.14 ± 0.12	1381 ± 70	0.276 ± 0.014	0.95 ± 0.04	4.29
L2	1100	10 987 ± 625	2.197 ± 0.125	1.52 ± 0.13	n. d.	n. d.	n. d.	3.31
L3	800	n. d.	n. d.	n. d.	n. d.	n. d.	n. d.	2.76
L4	20	n. d.	n. d.	n. d.	n. d.	n. d.	n. d.	3.20
L5	140	n. d.	n. d.	n. d.	n. d.	n. d.	n. d.	4.48
L6	1600	61 ± 4	0.012 ± 0.001	1.17 ± 0.10	962 ± 116	0.192 ± 0.023	0.86 ± 0.09	4.29
L7	200	n. d.	n. d.	n. d.	n. d.	n. d.	n. d.	2.85
L8	1000	545 ± 14	0.109 ± 0.003	1.02 ± 0.03	6516 ± 172	1.303 ± 0.034	0.80 ± 0.02	3.39
L9[b]	1200	600 ± 40	0.12 ± 0.01	0.68 ± 0.03	14 924 ± 1060	3.0 ± 0.2	0.67 ± 0.03	2.84
L10[c]	643	100	0.01	1.10 ± 0.05	3300	0.33	1.2 ± 0.2	5.69

[a] Determined through Virtual Computational Chemistry Laboratory. [b] Values taken from ref. 30. [c] Values taken from ref. 29. In some cases a reliable calculation of EC_{50} values was not possible (n. d.).

electrode and, at the end of the experiment (t = 300 s), a detergent was added to release all the encapsulated chloride anions. The obtained value was used to normalise the data. The assays were repeated using several concentrations. These data were fitted using Hill's equation, from which two parameters, EC_{50}, the concentration of the compound needed to induce 50% release of chloride anions, and n, the Hill parameter, were obtained. The lower the value of EC_{50}, the higher the potency of the anion carrier. Assays involving the exchange of Cl^- and NO_3^-, and of Cl^- and HCO_3^-, were conducted and the results are presented in Table 1. The chloride efflux promoted by the studied compounds at 5 μM concentration (5 μM, 1 mol% carrier to the lipid concentration) in unilamellar POPC vesicles in the of Cl^- and NO_3^- exchange assay is presented in Fig. 3. As expected, compounds **L1**, **L2**, **L6** and **L8**, containing a 7-indolyl residue, are those displaying the highest activity as chloride transporters. Nevertheless, significant differences depending on the nature of the other substituents were observed. Indeed, the presence of an alkyl chain as the substituent caused a remarkable reduction in the transport activity, and the EC_{50} value determined for **L2** is in the micromolar range (Cl^-/NO_3^- exchange), much higher than those calculated for compounds **L1**, **L8** and **L6**. **L1** and **L6**, containing aryl substituents bearing EWGs, are the most potent anion transporters of the family, outperforming the coumarin-substituted compound **L8**. **L6** bearing the 3,5-bis(trifluoromethyl) phenyl group was found to be the most active transporter, roughly two-fold as potent Cl^-/NO_3^- exchanger than **L1**, incorporating a 4-(pentafluorosulfanyl)phenyl residue. This trend is consistent with the number and nature of EWGs, especially when considering that both compounds display identical calculated lipophilicity values (Table 1).[32] Compounds **L3**, **L4**, **L5** and **L7** were found to display marginal transport activity and no EC_{50} value could be determined for these derivatives. The first three derivatives contain, at least, an indol-3-yl moiety attached to the squaramide core through an alkyl linker, whereas **L7** holds two indol-5-yl residues. Consequently, both aliphatic spacers and modification of the substitution position of the indole ring led to a dramatic decrease of the transport activity. This might be related to both the alkyl substitution of the squaramide N–H groups and the fact that the NH fragments of these indole moieties are not in a suitable position to interact with the anions as demonstrated by the ^{1}H NMR solution studies in DMSO-d_6/0.5% water. The EC_{50} values determined for the Cl^-/HCO_3^- exchange are, for a given compound, about one order of magnitude higher than those calculated for the Cl^-/NO_3^- exchange. This is commonly observed and is a consequence of the higher hydration energy of bicarbonate *vs.* nitrate, which makes the former more difficult to solubilise into the membrane than the latter. The trend observed for the studied compounds discussed above are as follows: **L6** is the most active transporter and **L2** is not active enough for the calculation of an accurate EC_{50}. It is interesting to compare the anionophoric properties of **L6** with respect to those previously observed for the symmetric 3,5-bis(trifluoromethyl)phenyl- and indol-7-yl-containing squaramides **L9** and **L10**.[28,30] **L6** was found to be ten-fold as potent than the bis-7-indolyl-containing squaramide **L9** in both Cl^-/NO_3^- and Cl^-/HCO_3^- exchange assays, whereas a similar potency to the symmetric bis(trifluoromethyl)phenyl-squaramide **L10** in the Cl^-/NO_3^- exchange experiment (EC_{50} 0.012 mol% *vs.* 0.01 mol%), and a small increase of potency in the Cl^-/HCO_3^- exchange assay (0.19 *vs.* 0.33 mol%) were observed. It can be speculated that the incorporation of an aromatic substituent bearing the EWG $-CF_3$ groups as well as the indol-7-yl residue provide an optimal balance of lipophilicity and hydrogen bond ability.

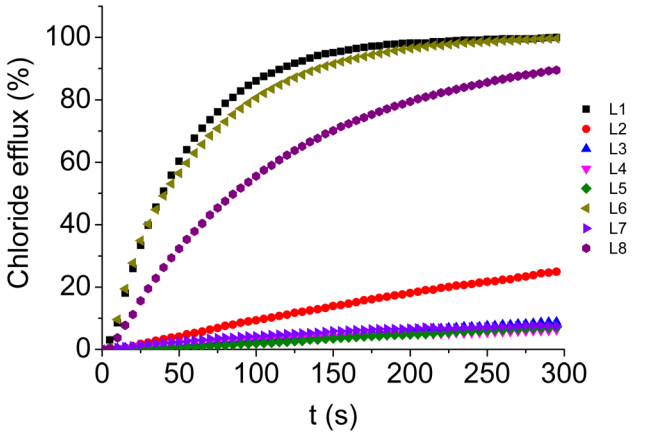

Fig. 3 Chloride efflux promoted by **L1–L8** (5 μM) in unilamellar POPC vesicles. Vesicles were loaded with a 489 mM NaCl solution buffered to pH 7.2 with 5 mM NaH_2PO_4 and dispersed in a 489 mM $NaNO_3$ solution buffered to pH 7.2 with 5 mM NaH_2PO_4. Each trace represents the average of at least three trials, performed with three batches of vesicles.

To check whether the activity exerted by these compounds was exclusively due to their anionophoric properties and not related to a detergent action, the well-known carboxyfluorescein-based experiment was carried out. Briefly, vesicles loaded with an aqueous solution containing NaCl and carboxyfluorescein, buffered to pH 7.2, were dispersed in an isotonic Na_2SO_4 aqueous solution, also buffered to pH 7.2. Emission changes were recorded over time upon the addition of the compound (t = 60 s) and, at the end of the assay, a detergent was added to lyse the vesicles and release all the entrapped carboxyfluorescein (t = 360 s). This led to a marked increase of emission intensity, which was used to normalise the data (for a thorough procedure see the ESI†). As observed in Fig. S88–S97,† addition of the studied compounds causes negligible emission changes, which allows us to conclude that none of them generates large non-selective pores in the membrane and, consequently, that their activity is only due to their ability to exchange anions throughout the membrane.

The ability of these squaramides to discharge pH gradients across the membrane was also evaluated by means of the HPTS-based assay.[33] 7 : 3 POPC:cholesterol vesicles were hydrated with an aqueous solution containing $NaNO_3$ and HPTS (a ratiometric fluorescent probe which is also sensitive to pH changes), buffered to pH 7.2, and suspended in an isotonic $NaNO_3$ aqueous solution buffered to pH 7.2 as well. A pH

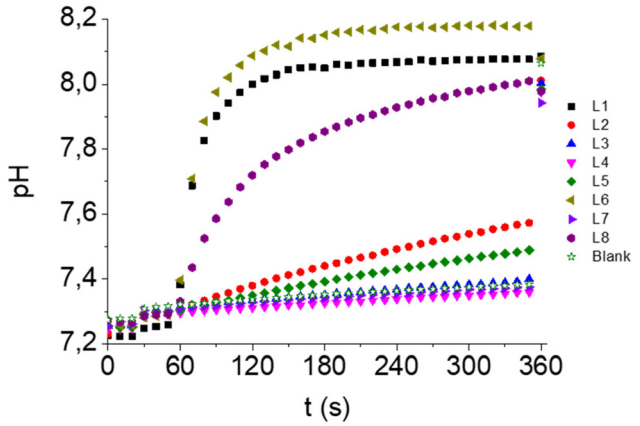

Fig. 4 Variation of pH upon addition of compounds **L1–L8** (0.5 μM) to 7 : 3 POPC:cholesterol vesicles (0.5 mM POPC). Vesicles (loaded with a 126.2 mM $NaNO_3$ solution buffered to pH 7.2 with 10 mM NaH_2PO_4, and containing 1 mM HPTS; ionic strength (I.S.) 150 mM), were suspended in a $NaNO_3$ solution (126.2 mM $NaNO_3$ buffered to pH 7.2 with 10 mM NaH_2PO_4; I.S. 150 mM). At t = 30 s an aliquot of a NaOH solution (12.5 μL, 0.5 M) was added, and at t = 60 s the anion carrier was added. The blank is DMSO (1.25 μL). Each trace represents the average of at least three trials, performed with three batches of vesicles.

gradient was created by adding an aliquot of a NaOH aqueous solution (t = 30 s), followed by the addition of the compound (t = 60 s). Changes in the I_{460}/I_{403} ratio were monitored over time and the experiment was finished by adding a detergent (t = 360 s). The obtained emission ratios were subsequently converted to pH values through calibration (see ESI for details†). As observed in Fig. S98–S105,† the ability of the studied squaramides to dissipate the pH gradient depends on their concentration. As shown in Fig. 4, the most active compounds, **L1**, **L6** and **L8**, are found to balance the pH at 0.5 μM concentration, whereas **L2** and **L5** display a poor activity and **L3**, **L4** and **L7** are not active under these conditions. This trend is very similar to that observed in the ISE assays and confirms the importance of both the lipophilicity and the substitution pattern of the squaramides (including the presence or absence of EWGs in the molecule backbone) in the transport activity.

Conclusions

In conclusion, we have studied a novel family of squaramide-based compounds **L1–L8**, with the aim to evaluate the effect of the indolyl substituent on their anion binding and transmembrane anion transport properties. ^{1}H NMR titration experiments conducted in DMSO-d_6/0.5% water solution showed a stronger affinity of **L1**, **L2**, **L6**, and **L8**, bearing an indol-7-yl residue, towards the chloride anion, forming 1 : 1 anion adducts, and confirming that the presence of an additional H-bond donor group improves their anion binding affinities. These observations were also supported by the solid state structure of the **L6** chloride complex. **L1**, **L6**, and **L8** are also the most potent anion transporters of the family. They are also able to dissipate a roughly 1.0 unit pH gradient across the membrane at 0.5 μM concentration. The other compounds exhibit a significantly lower activity or are not active. Importantly, the anion transport potency of L6 is favourably comparable with that of their symmetrically substituted parent squaramides. Indeed, **L6** displayed an EC_{50} value ten-fold lower than that of its bis 7-indolyl squaramide analogue **L9**, and comparable to or slightly lower than those previously reported for the symmetric analogue with 3,5-bis(trifluoromethyl)phenyl residues **L10**. This piece of work highlighted how additional H-bond donor groups, due to the presence of the 7-indolyl residue in this case, could be used in combination with the presence or absence of electron-withdrawing groups in their structures to control the anion binding strength and lipophilicity with the aim to improve their anion binding and transmembrane anion transport properties, and to obtain potent anionophores.

Author contributions

Conceptualisation: CC, RQ. Writing – original draft: GP, IC-B. Writing – review and editing: CC, RQ, GP, IC-B. Investigation: GP, IC-B, JM, CB, DA-C. Data curation: GP, IC-B. Visualisation: GP, IC-B. Funding acquisition: CC, RQ.

Conflicts of interest

There are no conflicts to declare.

Acknowledgements

This research has been financially supported by the Consejería de Educación de la Junta de Castilla y León (project BU067P20) and the Ministerio de Ciencia e Innovación (project PID2020-117610RB-I00). I. C.-B. and D. A.-C. thank the Consejería de Educación de la Junta de Castilla y León, the European Social Fund (ESF) and the European Regional Development Fund (ERDF) for their post-doctoral (I. C.-B.) and pre-doctoral (D. A.-C.) contracts. The authors gratefully acknowledge Andrea Sancho-Medina for her contributions to transmembrane anion transport experiments. Financial support from MIUR (PRIN 2017 project 2017EKCS35) is gratefully acknowledged by C. C. and G. P. along with the Università degli Studi di Cagliari (FIR 2016-2019) and the Fondazione di Sardegna (FdS Progetti Biennali di Ateneo, annualità 2020, project F75F21001260007).

References

1 R. Benz and R. E. W. Hancock, *J. Gen. Physiol.*, 1987, **89**, 275–295.
2 C. Duran, C. H. Thompson, Q. Xiao and H. C. Hartzell, *Annu. Rev. Physiol.*, 2009, **72**, 95–121.

3 F. M. Ashcroft, *Ion Channels and Disease*, Academic Press, 2000.
4 J. S. Elborn, *Lancet*, 2016, **388**, 2519–2531.
5 C. Castellani and B. M. Assael, *Cell. Mol. Life Sci.*, 2017, **74**, 129–140.
6 M. Shteinberg, I. J. Haq, D. Polineni and J. C. Davies, *Lancet*, 2021, **397**, 2195–2211.
7 H. Li, J. J. Salomon, D. N. Sheppard, M. A. Mall and L. J. Galietta, *Curr. Opin. Pharmacol.*, 2017, **34**, 91–97.
8 H. Li, H. Valkenier, A. G. Thorne, C. M. Dias, J. A. Cooper, M. Kieffer, N. Busschaert, P. A. Gale, D. N. Sheppard and A. P. Davis, *Chem. Sci.*, 2019, **10**, 9663–9672.
9 R. Quesada and R. Dutzler, *J. Cystic Fibrosis*, 2020, **19**, S37–S41.
10 A. Gianotti, V. Capurro, L. Delpiano, M. Mielczarek, M. García-Valverde, I. Carreira-Barral, A. Ludovico, M. Fiore, D. Baroni, O. Moran, R. Quesada and E. Caci, *Int. J. Mol. Sci.*, 2020, **21**, 1488.
11 G. Picci, S. Marchesan and C. Caltagirone, *Biomedicines*, 2022, **10**, 885.
12 V. Kaushik, J. Yakisich, A. Kumar, N. Azad and A. Iyer, *Cancers*, 2018, **10**, 360.
13 L. Tapia, Y. Pérez, M. Bolte, J. Casas, J. Solá, R. Quesada and I. Alfonso, *Angew. Chem., Int. Ed.*, 2019, **58**, 12465–12468.
14 S.-H. Park, S.-H. Park, E. N. W. Howe, J. Y. Hyun, L.-J. Chen, I. Hwang, G. Vargas-Zuñiga, N. Busschaert, P. A. Gale, J. L. Sessler and I. Shin, *Chem*, 2019, **5**, 2079–2098.
15 J. T. Davis, P. A. Gale and R. Quesada, *Chem. Soc. Rev.*, 2020, **49**, 6056–6068.
16 A. I. Share, K. Patel, C. Nativi, E. J. Cho, O. Francesconi, N. Busschaert, P. A. Gale, S. Roelens and J. L. Sessler, *Chem. Commun.*, 2016, **52**, 7560–7563.
17 I. Carreira-Barral, C. Rumbo, M. Mielczarek, D. Alonso-Carrillo, E. Herran, M. Pastor, A. Del Pozo, M. García-Valverde and R. Quesada, *Chem. Commun.*, 2019, **55**, 10080–10083.
18 R. Herráez, R. Quesada, N. Dahdah, M. Viñas and T. Vinuesa, *Pharmaceutics*, 2021, **13**, 705.
19 M. A. Scorciapino, G. Picci, R. Quesada, V. Lippolis and C. Caltagirone, *Membranes*, 2022, **12**, 292.
20 V. Saggiomo, S. Otto, I. Marques, V. Félix, T. Torroba and R. Quesada, *Chem. Commun.*, 2012, **48**, 5274–5276.
21 N. J. Knight, E. Hernando, C. J. E. Haynes, N. Busschaert, H. J. Clarke, K. Takimoto, M. García-Valverde, J. G. Frey, R. Quesada and P. A. Gale, *Chem. Sci.*, 2016, **7**, 1600–1608.
22 L. Martínez-Crespo, L. Halgreen, M. Soares, I. Marques, V. Félix and H. Valkenier, *Org. Biomol. Chem.*, 2021, **19**, 8324–8337.
23 X. Wu, J. R. Small, A. Cataldo, A. M. Withecombe, P. Turner and P. A. Gale, *Angew. Chem., Int. Ed.*, 2019, **58**, 15142–15147.
24 J. Yang, G. Yu, J. L. Sessler, I. Shin, P. A. Gale and F. Huang, *Chem*, 2021, **7**, 3256–3291.
25 N. Busschaert, S. J. Bradberry, M. Wenzel, C. J. E. Haynes, J. R. Hiscock, I. L. Kirby, L. E. Karagiannidis, S. J. Moore, N. J. Wells, J. Herniman, G. J. Langley, P. N. Horton, M. E. Light, I. Marques, P. J. Costa, V. Félix, J. G. Frey and P. A. Gale, *Chem. Sci.*, 2013, **4**, 3036–3045.
26 B. A. McNally, A. V. Koulov, T. N. Lambert, B. D. Smith, J.-B. Joos, A. L. Sisson, J. P. Clare, V. Sgarlata, L. W. Judd, G. Magro and A. P. Davis, *Chem.– Eur. J.*, 2008, **14**, 9599–9606.
27 N. Busschaert, R. B. P. Elmes, D. D. Czech, X. Wu, I. L. Kirby, E. M. Peck, K. D. Hendzel, S. K. Shaw, B. Chan, B. D. Smith, K. A. Jolliffe and P. A. Gale, *Chem. Sci.*, 2014, **5**, 3617–3626.
28 N. Busschaert and P. A. Gale, *Angew. Chem., Int. Ed.*, 2013, **52**, 1374–1382.
29 N. Busschaert, I. L. Kirby, S. Young, S. J. Coles, P. N. Horton, M. E. Light and P. A. Gale, *Angew. Chem., Int. Ed.*, 2012, **51**, 4426–4430.
30 G. Picci, M. Kubicki, A. Garau, V. Lippolis, R. Mocci, A. Porcheddu, R. Quesada, P. C. Ricci, M. A. Scorciapino and C. Caltagirone, *Chem. Commun.*, 2020, **56**, 11066–11069.
31 M. J. Hynes, *J. Chem. Soc., Dalton Trans.*, 1993, 311–312.
32 **https://www.vcclab.org**(last access: April 2022).
33 A. M. Gilchrist, P. Wang, I. Carreira-Barral, D. Alonso-Carrillo, X. Wu, R. Quesada and P. A. Gale, *Supramol. Chem.*, 2021, **33**, 325–344, DOI: **10.1080/10610278.2021.1999956**.